

pubs.acs.org/JPCA Article

The Photoionization Time in π -Conjugated Molecular Systems

Deep Mukherjee, Shaul Mukamel, and Upendra Harbola*



Cite This: J. Phys. Chem. A 2020, 124, 5770-5774



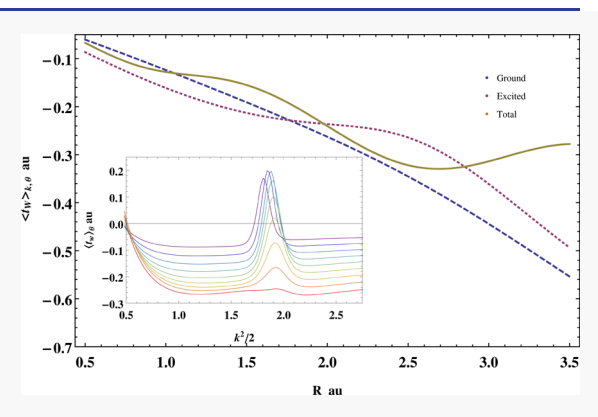
ACCESS I

III Metrics & More



s Supporting Information

ABSTRACT: The photoionization time of C_2H_4 is calculated as a model for π -conjugated molecular systems. Analytical results are obtained using the Wigner phase delay, which is compared with energy-streaking measurements. We find that, although the ionization time averaged over nuclear configurations compares well in the two measures, the dependence on the nuclear configuration is different. Interference between different ionization pathways depends significantly on the molecular geometry and the ionizing electron energy and may lead to qualitative changes in the ionization time.



Recently developed extreme ultraviolet (XUV) attosecond pulses have enabled the study of the electron dynamics and photoionization times in atoms, molecules, and clusters. ^{1–4} In experiment, an attosecond XUV pulse is used to ionize an electron. A subcycle oscillation of high-intensity IR laser pulse is then used to streak the photoionized electron. ^{1,5,6} Depending on when the ionized electron enters the free state, its dynamics and energy are governed by the IR field. The change in photoelectron spectra with the time delay between the XUV and IR pulses allows to estimate the ionization times in atoms. ⁷ Other experimental techniques, such as the attoclock technique, ^{8,9} and reconstruction of attosecond beating by interference of two-photon transition (RABBIT), ¹⁰ have also been employed to extract the ionization time delay. ^{4,11,12}

Several theoretical approaches have been used to describe laser-assisted ionization processes ^{13,14} in atoms and molecules ¹⁵ (see also ref 16 and the references therein). Various definitions have been proposed for the ionization time. These include Larmor time, Buttiker time, Pollock—Miller time, and Wigner time. ¹⁷ In a recent work, ¹⁸ a Bohmian tunneling time, which corresponds to the time that Bohmian trajectory spends in a classically forbidden region, has been introduced. However, it was found that this time was several orders of magnitude longer than the experimentally obtained ionization time.

The photoionization process in molecules is more challenging than in atoms. What sets a molecule apart is the vibrational degrees of freedom, which may couple strongly to the electron dynamics. Although during ionization the electrons effectively experience a static nuclear force, a statistical disorder of nuclear configurations may have a significant effect on the ionization times. The static nuclear

heterogeneity has also been shown to affect charge migration in molecules. Here, we calculate the Wigner ionization time 20,21 for linear π -conjugated molecules. Our primary goal is to study the effect of the nuclear configuration on ionization time using an analytically tractable model. We compare the Wigner ionization time with the one estimated from the energy streaking spectrogram obtained by using an IR laser pulse. The two methods show different dependence on the nuclear configuration. However, upon averaging over molecular configurations, the ionization times from both methods are found to agree well.

We study the ionization time of ethylene (C_2H_4) using the Hückel model. This simple model allows us to derive approximate analytical expressions. We take the molecular bond axis along z, and the carbons are sp^2 -hybridized. The valence electron dynamics can be treated by only considering the π electrons and neglecting the σ electrons. The core electrons and the σ electrons, which bind the two nuclei, are treated within the mean-field approximation via screened nuclear charge as seen by the π electrons. The π electrons are assumed to only experience an effective nuclear charge, which represents the σ and core electrons. Such treatment has been quite successful in describing molecular valence orbitals. The model represents a two-particle π -electron fermionic system in an effective potential having cylindrical symmetry along the z

Received: June 13, 2020 Published: June 17, 2020





axis. We treat the nuclear motion of the two C atoms as a harmonic oscillator.

We start with the molecular Hamiltonian, $H_{\rm M}=H_{\pi}+H_{\sigma}+H_{\sigma-\pi}$, where H_{π} represents the π electrons, H_{σ} denotes the σ -bonded molecular backbone, and $H_{\sigma-\pi}$ denotes the interaction between H_{π} and H_{σ} . $H_{\pi}+H_{\sigma-\pi}$ can be written as

$$H_{\pi} + H_{\sigma - \pi} = \frac{1}{2} \nabla_{1}^{2} - \frac{1}{2} \nabla_{2}^{2} - \frac{z^{*}}{r_{1}} - \frac{z^{*}}{r_{2}} + \frac{1}{|\mathbf{r_{1}} - \mathbf{r_{2}}|} - \frac{z^{*}}{|\mathbf{r_{1}} - \mathbf{R}|} - \frac{z^{*}}{|\mathbf{r_{2}} - \mathbf{R}|}$$
(1)

where 1 and 2 are the π -electron indices and R is the bond length. Boldface letters represent vectors, and \mathbf{r}_1 and \mathbf{r}_2 are the positions of two electrons with respect to nucleus A (Figure 1 in the Supporting Information). z^* denotes the effective nuclear charge felt by π electrons. The first two terms in the right-hand side of eq 1 denote the kinetic energy of the π electrons, and the following two terms are the potential energies due to nucleus A. The two-electron term represents the repulsive potential energy between the π electrons, and the remaining terms represent attractive potential energy between the π electrons and nucleus B. We assume the harmonic potential created by the σ and core electrons:

$$H_{\sigma} = -\frac{1}{2}\nabla_{R}^{2} + \frac{1}{2}\kappa(R - R_{0})^{2} - V \tag{2}$$

which depends on the parameters κ , R_0 , and V. H_σ represents the di-cationic system C_2^{2+} . Parameters κ and V and z^* are obtained from quantum chemistry calculation on the ionized system as discussed in the Supporting Information. The total Hamiltonian represents the neutral system whose bound and scattering states are obtained in the Supporting Information.

The XUV pulse interacts with the bound-state π electrons, forcing an electron to move away from the nuclei. Within the dipole approximation, the interaction $(H_{\rm int})$ of the XUV electric field with the molecule is $H_{\rm int} = -\mathbf{E}(t) \cdot \hat{\mu}$, where $\mathbf{E}(t)$ is the optical electric field and $\hat{\mu} = e \cdot \sum_{i=1,2} \hat{\mathbf{r}}_i$ is the dipole moment operator. The dipole coupling between the neutral ground and the scattering state facilitates the ionization process. If ionization is instantaneous and independent of electron energy, the ionizing electron wave packet is identical to the XUV extra phase in the photoelectron wave packet. This phase provides a measure of the time delay of the electronic response to the interaction with the XUV field. The time-dependent molecular wave packet is given by

$$|\Psi(t)\rangle = -i \int_{t0}^{t} dt' e^{-i \int_{t'}^{t} dt'' H(t'')} H_{XUV}(t') e^{-i H_{M}(t'-t_{0})} |\Phi\rangle$$

$$+ e^{-i H_{M}(t-t_{0})} |\Phi\rangle$$
(3)

Equation 3 is the exact solution of the Schrodinger equation for the scattered molecular wave packet created by the XUV pulse. Since the XUV field is weak, we compute the time-dependent photoelectron wave packet, eq 3, by first-order perturbative approximation. This is equivalent to replacing H by $H_{\rm M}$ in eq 3.

The scattered electron wave-packet amplitude in the kth scattered state is obtained by projecting the scattering state onto $|\Psi(t)\rangle$. For the present calculation, we assume that the XUV field is a Gaussian pulse¹⁶ with carrier frequency $\omega_{\rm X}$ polarized along the molecular axis (\hat{z}) , $E_{\rm x}(t)=\hat{z}\mathcal{E}_0{\rm e}^{-at^2-i\omega_{\rm X}t}$,

where $\left(a=\frac{2\ln(2)}{\tau_{\text{XUV}}^2}\right)$ and τ_{XUV} , and \mathcal{E}_0 denote the duration and the amplitude of the XUV pulse, respectively. Photoelectron spectra are usually measured long after the XUV field has passed when the electron is free. In the $t \to \infty$ limit, we obtain

$$\Psi_{k} = -i \sum_{I=L,H} \hat{z} \cdot \mu_{I}(\mathbf{k}) \mathcal{E}_{0} e^{-(\omega_{X} - (k^{2}/2) + E_{0} - E_{I})^{2}/4a}$$
(4)

where $\mu_{\rm I}({\bf k})$ is the dipole matrix element between the scattering (denoted with index ${\bf k}$) and the neutral ground states of the molecule. More details are given in the Supporting Information. I = H, L stands for the HOMO(H) and LUMO(L) for the cation. The wave packet contains contributions from both the ground (I = H) and the excited (I = L) cationic states. E_0 denotes the energy of the neutral ground state, and $E_{\rm I}$ are the energies of the cationic states. The difference $E_0-E_{\rm H}$ represents the ionization energy for the π orbital. For model parameters (V, κ , z^*), this ionization energy can be computed from Eqs (10a) and (26) in the Supporting Information. At equilibrium (R=2.19 au), the ionization energy is found to be 10.43 eV, which is in good agreement with quantum chemistry calculation reported in ref 23 and experiments. 24,25

The Wigner ionization time delay is then computed as $t_{\rm W}(\mathbf{k},R)=\frac{1}{k}\frac{\partial {\rm arg}(\Psi_{\rm k}(\mathbf{k}))}{\partial k}$ where k is the free-electron kinetic momentum. The ground and excited states of the cation provide two pathways for the ionization process. The Wigner ionization times associated with these two pathways are different. If $t_{\rm W_H}(\mathbf{k},R)$ and $t_{\rm W_L}(\mathbf{k},R)$ are the Wigner times for the ground and excited cationic states, respectively, the net ionization time, $t_{\rm W}(\mathbf{k},R)$, can be expressed as (see Eqs (63)–(69) in the Supporting Information for derivation)

$$t_{W}(\mathbf{k}, R) = \frac{t_{W_{H}} + \chi^{2} t_{W_{L}} \frac{u_{L}^{2} + v_{L}^{2}}{u_{H}^{2} + v_{H}^{2}} + \frac{\chi[u_{L}v'_{H} - u'_{L}v_{H} + v_{L}u'_{H} - v'_{L}u_{H}]}{k(u'_{H}^{2} + v_{H}^{2})} + \frac{\chi'[u_{L}v_{H} - v_{L}u_{H}]}{k(u_{H}^{2} + v_{H}^{2})}}{1 + \chi^{2} \frac{u_{L}^{2} + v_{L}^{2}}{u_{H}^{2} + v_{H}^{2}} + 2\chi \frac{u_{H}u_{L} + v_{H}v_{L}}{u_{H}^{2} + v_{H}^{2}}}$$
(5)

where $t_{W_H}(\mathbf{k}, R) = \frac{1}{k} \frac{v_H u_H' - u_H v_H'}{v_H^2 + u_H^2}$, $t_{W_L}(\mathbf{k}, R) = \frac{1}{k} \frac{v_L u_L' - u_L v_L'}{v_L^2 + u_L^2}$, and $u_{H(L)}/v_{H(L)}$ are defined in Eqs (66)–(69) in the Supporting Information. χ' , $u_{H(L)}'$, and $v_{H(L)}'$ denote the derivative of χ , $u_{H(L)}'$, and $v_{H(L)}$ with respect to k, and

$$\chi = \sqrt{\frac{1 + S(R)}{1 - S(R)}} \frac{D_{L}(R)}{D_{H}(R)} \frac{e^{-(\omega_{X} - (k^{2}/2) + E_{0} - E_{L})^{2}/4a}}{e^{-(\omega_{X} - (k^{2}/2) + E_{0} - E_{H})^{2}/4a}}$$
(6)

Equation 5 together with eq 6 is our main result. The parameter χ controls the relative weight of the two pathways in the ionization process. The overlap function, S(R), and the Dyson orbital coefficients, $D_{\rm H/L}(R)$, for the ground/excited cationic states are given in Eqs (32) and (33) in the Supporting Information. χ decreases with increasing k, indicating that the excited state pathway contribution diminishes as k is increased. This is due to energy conservation; for a given XUV photon energy, the ground state pathway leaves the ionized electron in a higher energy scattering state as compared to via the excited state pathway where the cation energy is higher. Hence, for smaller values of k, where χ is large, one expects $t_{\rm W}(\mathbf{k},R) \approx t_{\rm W_L}(\mathbf{k},R)$, while for larger values of k, χ is small and $t_{\rm W}(\mathbf{k},R) \approx t_{\rm W_L}(\mathbf{k},R)$. For

intermediate k values, both pathways contribute significantly to $t_{\rm W}(\mathbf{k},R)$, resulting in interesting interference effects. Note that $t_{\rm W}(\mathbf{k},R)$ depends on both the magnitude and the direction of the wave vector \mathbf{k} , which makes an angle θ with the molecular axis. $t_{\rm W}(\mathbf{k},R)$ is an antisymmetric function of θ around $\theta=\pi/2$ for a given value of k, while the probability density of scattering into an angle θ and $\theta+\mathrm{d}\theta$ is symmetric (Figure 2 in the Supporting Information). This symmetry is due to the symmetry of the eigenstates of the Hamiltonian H. Thus, forward scattering ($0<\theta<\pi/2$) probability into an angle θ with ionization time τ is the same as scattering into the angle $\theta+\pi/2$ with ionization time $-\tau$. We define the average ionization time in the forward direction $\langle t_{\rm W}(\mathbf{k},R) \rangle_{\theta,k}$ by integrating over all forward angles and k values. This time is plotted in Figure 1 for varying distance between the

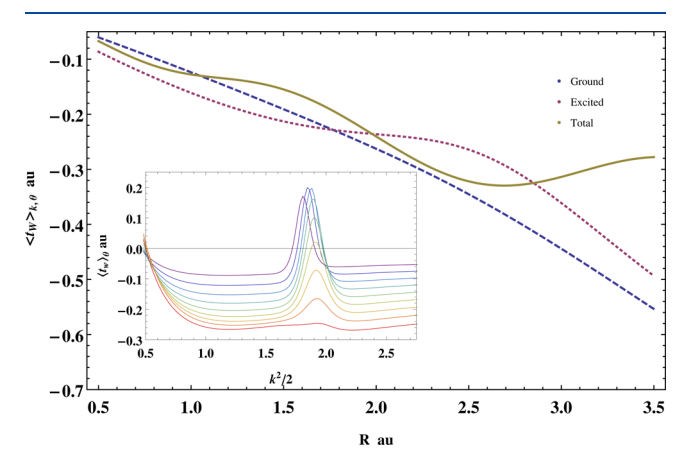


Figure 1. Wigner ionization time $\langle t_{\rm W} \rangle_{\theta,\,k}$ (solid curve) as function of the bond length, R, in atomic units. Dashed curve represents $\langle t_{\rm W_H} \rangle_{\theta,\,k}$ and dotted curve denotes $\langle t_{\rm W_L} \rangle_{\theta,\,k}$. The inset shows variation in $\langle t_{\rm W} \rangle_{\theta}$ with the kinetic energy of the ionized electron for different values of R=2.1 to 0.5 in steps of 0.2 from bottom to top. The effective nuclear charge $z^*=1.8$ au (neutral) and 2.2 au (cation).

carbon atoms. This average ionization time is found to be negative for all *R* values considered, indicating that the ionized electron wave packet in the forward direction precedes the XUV pulse. However, the averaged ionization time,

 $\langle t_{\rm W}({\bf k},\,R)\rangle_{\theta}$, in the forward direction is very sensitive to the scattered electron energy and shows qualitative differences as compared to $\langle t_{\rm W}({\bf k},R)\rangle_{\theta,\,k}$ as R is varied. This is shown in the inset of the figure. As R is decreased, interference between the two pathways, which is significant at intermediate values of the electron kinetic energy, increases and manifests itself in a peak-like structure in $\langle t_{\rm W}({\bf k},\,R)\rangle_{\theta}$. This results in a positive ionization time in the forward direction for smaller values of R at intermediate energies.

Finally, the molecular vibration different molecules in the gas may have a statistical distribution over different nuclear configurations during interaction with the XUV pulse. For a harmonic vibration, the distribution in R is given by $f(R) = \sqrt{\frac{\kappa}{\omega \pi}} \mathrm{e}^{-\kappa/\omega(R-R_0)^2}$, corresponding to the ground eigenstate probability density of H_σ . ω and κ are the corresponding frequency and force constant of the vibration. The parameters in H_σ are obtained by quantum chemistry calculation using Gaussian 09. Force constant (κ) = 1.38 au, $R_0 = 2.19$ au, and $\bar{\lambda} = \frac{\omega}{2\pi c} = 1050$ cm⁻¹ are obtained from quantum chemistry calculation of C_2^{2+} . c denotes the speed of light in vacuum. We therefore define an average Wigner time, $\langle \tau_W \rangle_R$, by taking the average over the bond length as $\langle \tau_W \rangle_R = \int \mathrm{d}R f(R) \langle t_W \rangle_{\theta_0}$, k We find $\langle \tau_W \rangle_R = 0$. 27 au or 6.5 as.

We next discuss the ionization time as probed in the attosecond energy streaking experiment. In the streaking measurement, after ionization, a strong IR field drags the free electron to different momentum states. The quantity of interest in this case is the streaking spectrogram, which is a series of photoelectron spectra for varied time delay between XUV and IR pulses. To obtain this distribution, we first compute the amplitude of the ionized electron to be in one of the scattering states. In the presence of the IR pulse, eq 3 represents the exact scattering wave packet due to interaction with XUV and IR where we replace $H(t) = H_M + H_F(t) +$ $H_X(t)$, $H_{IR}(t)$ and $H_X(t)$ represent the interaction of the molecular system with IR and XUV fields, respectively. Since the IR pulse interacts with the electron wave packet only after it reaches the scattering state, the corresponding wave packet at time t acquires a phase $e^{i(\mathbf{A}(t)-\mathbf{A}(t'))}$, where $\mathbf{A}(t)$ is the vector potential of the IR field and t' is the time when the electron wave packet starts to interact with the IR field. The

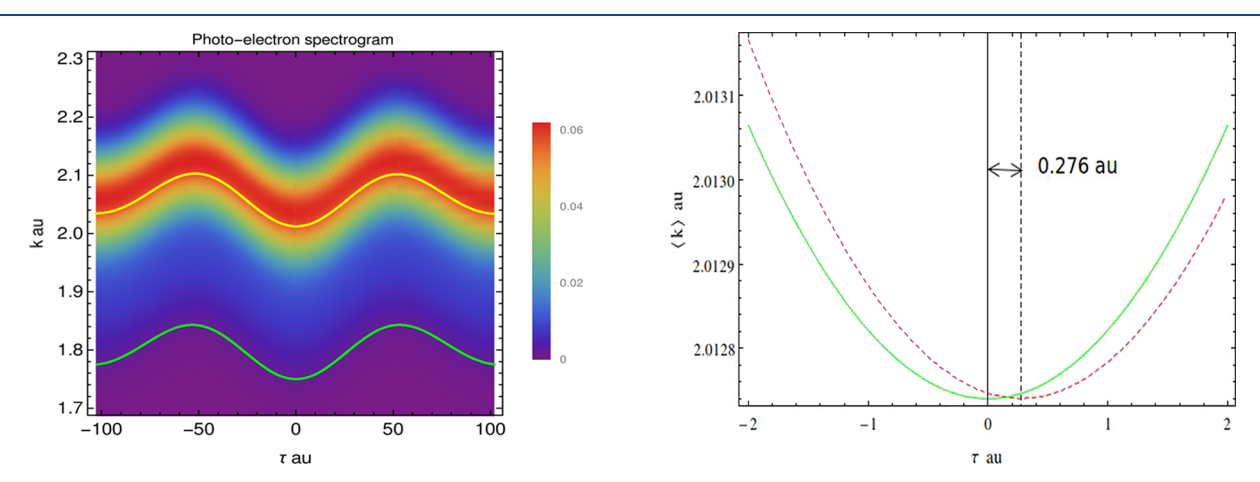


Figure 2. (Left panel) Attosecond streaking spectrogram for ethylene at R = 2.19 au in the presence of vector potential $A(t) = 0.5 \cos^2\left(\frac{0.057t}{8}\right) \cos(0.057t)$ au. Yellow and green solid curves show the average momentum and the vector potential, respectively. (Right panel) Average momentum (dashed red line) and IR vector potential (solid green line) vs the XUV-IR delay.

effect of the IR field can be incorporated by dressing the scattering states with the vector potential as detailed in Eq (72) in the Supporting Information.

The photoelectrons are collected at the detector at long time T (much longer than the IR field period), when the IR field is switched off. To obtain the photoelectron spectra at long time T, we calculate the amplitude by projecting the scattering state onto $|\Psi(T)\rangle$:

$$\Psi(\mathbf{p}, R) = -i \sum_{I} \int_{t_0}^{T} dt e^{-i \int_{t}^{T} (\mathbf{p} + \mathbf{A}(t''))^2 / 2 dt'' - i E_{I}(T - t)}$$

$$\mathbf{E}_{\mathbf{X}}(t) \cdot \mu_{\mathbf{I}\mathbf{p}}(t) e^{i E_{0}(t - t_0)}$$
(7)

where ${\bf p}$ is the free electron canonical momentum. The photoelectron spectrum is given by $|\Psi_{\bf p}(R)|^2$. Since the final time, T, is not measured (the detector only resolves energy), we average the wave packet over this long time. Using this time averaged wave packet, we have computed the average kinetic momentum of the photoelectrons for various delay, τ , between the XUV field and IR vector potential. If the ionization process is instantaneous, the average kinetic momentum should change with τ in phase with the IR vector potential; the relative phase delay between them is then a measure of the ionization time.

Numerically evaluated attosecond streaking spectra averaged over all angles, $\langle |\Psi(\tau,k)|^2 \rangle_{\theta}$, are shown in Figure 2 with varying delay (τ) and kinetic momentum k at equilibrium R=2.19 au. The average kinetic momentum (yellow solid line) follows the vector potential (green solid line). The phase delay between the two corresponds to ionization time of -0.276 au (-6.65 as). The time is negative because the phase of the kinetic momentum of the ionized electron precedes the vector potential.

When the ionization time is obtained from the streaking spectrogram at different values of R, we find that it shows an overall non-monotonic increasing trend over the range of R values as shown in Figure 3. Note that the ionization times for individual pathways show a very different dependence on R. The ionization time due to the excited (ground) state pathway decreases (increases) as R is increased. The variation of the overall ionization time is similar to the ground state pathway. This R dependence is however different from the Wigner time

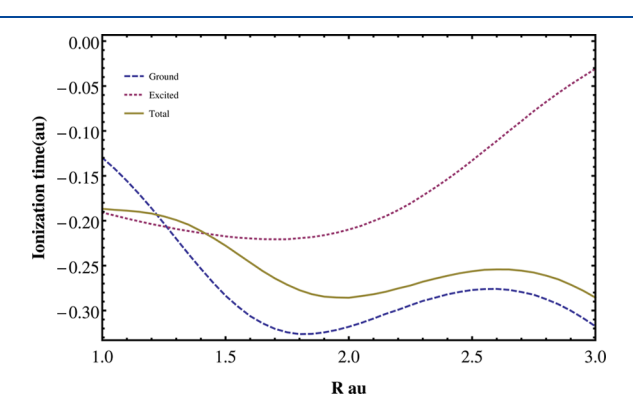


Figure 3. Ionization time vs interatomic distance as obtained from the streaking spectrogram. The dashed and dotted curves represent the ionization time when only the ground or the excited cationic state pathway contributes to ionization. The solid curve shows the net ionization time when both pathways contribute to the ionization process.

in Figure 1. Although, when averaged over the distribution, f(R), the average ionization time delay is found to be -0.28 au (-0.677 as), which is almost the same as average Wigner time.

In conclusion, we have analyzed the bond-length effect on the ionization time in C_2H_4 . Even though nuclei remain almost frozen during the fast ionization process, the statistical distribution of bond lengths can still affect the ionization time. The Wigner scattering time and the energy streaking method show different dependence on the bond length. However, when averaged over the distribution of bond lengths, both methods give similar ionization times. This is because the ionization time at the equilibrium configuration of nuclei is found to be the same in both approaches. Here, for simplicity, we have considered ionization only from the π molecular orbital (1b₃₁₁). However the ionization from other orbitals, such as $1b_{3g}$, $3a_g$, and $1b_{2w}$ can also take place²³ using the XUV pulse considered here. We expect to have maximum ionization from the π orbital since it has the least ionization energy. Here, we have assumed zero temperature. It will be interesting to study finite temperatures involving excited vibrational states.

ASSOCIATED CONTENT

Supporting Information

The Supporting Information is available free of charge at https://pubs.acs.org/doi/10.1021/acs.jpca.0c05369.

Essential mathematical steps and results that are used to derive the Wigner ionization time in Eq. (5) of the main text are described. (PDF)

AUTHOR INFORMATION

Corresponding Author

Upendra Harbola — Department of Inorganic and Physical Chemistry, Indian Institute of Science, Bangalore 560012, India; Orcid.org/0000-0003-4053-8641; Phone: (+91) 080 2293 3410; Email: uharbola@iisc.ac.in

Authors

Deep Mukherjee — Department of Inorganic and Physical Chemistry, Indian Institute of Science, Bangalore 560012, India Shaul Mukamel — Department of Chemistry, Physics and Astronomy, University of California, Irvine, Irvine, California 92614, United States; Occid.org/0000-0002-6015-3135

Complete contact information is available at: https://pubs.acs.org/10.1021/acs.jpca.0c05369

Notes

The authors declare no competing financial interest.

ACKNOWLEDGMENTS

U.H. acknowledges financial support from the Science and Engineering Board (SERB), India, under grant EMR/2016/001280. S.M. gratefully acknowledges the support of the NSF through grant CHE-1953045.

REFERENCES

- (1) Kienberger, R.; Goulielmakis, E.; Uiberacker, M.; Baltuska, A.; Yakovlev, V.; Bammer, F.; Scrinzi, A.; Westerwalbesloh, T.; Kleineberg, U.; Heinzmann, U.; Drescher, M.; Krausz, F. Atomic transient recorder. *Nature* **2004**, *427*, 817–821.
- (2) Schultze, M.; et al. Delay in photoemission. *Science* **2010**, 328, 1658–1662.
- (3) Cavalieri, A. L.; Müller, N.; Uphues, T.; Yakovlev, V. S.; Baltuška, A.; Horvath, B.; Schmidt, B.; Blümel, L.; Holzwarth, R.;

- Hendel, S.; Drescher, M.; Kleineberg, U.; Echenique, P. M.; Kienberger, R.; Krausz, F.; Heinzmann, U. Attosecond spectroscopy in condensed matter. *Nature* **2007**, *449*, 1029–1032.
- (4) Huppert, M.; Jordan, I.; Baykusheva, D.; von Conta, A.; Wörner, H. J. Attosecond delays in molecular photoionization. *Phys. Rev. Lett.* **2016**, *117*, No. 093001.
- (5) Itatani, J.; Quéré, F.; Yudin, G. L.; Ivanov, M. Y.; Krausz, F.; Corkum, P. B. Attosecond streak camera. *Phys. Rev. Lett.* **2002**, *88*, 173903.
- (6) Drescher, M.; Hentschel, M.; Kienberger, R.; Tempea, G.; Spielmann, C.; Reider, G. A.; Corkum, P. B.; Krausz, F. X-ray pulses approaching the attosecond frontier. *Science* **2001**, *291*, 1923–1927.
- (7) Nagele, S.; Pazourek, R.; Feist, J.; Doblhoff-Dier, K.; Lemell, C.; Tőkési, K.; Burgdörfer, J. J. Phys. B: At., Mol. Opt. Phys. 2011, 44, No. 081001
- (8) Torlina, L.; Morales, F.; Kaushal, J.; Ivanov, I.; Kheifets, A.; Zielinski, A.; Scrinzi, A.; Muller, H. G.; Sukiasyan, S.; Ivanov, M.; Smirnova, O. Interpreting attoclock measurements of tunnelling times. *Nat. Phys.* **2015**, *11*, 503.
- (9) Sainadh, U. S.; Xu, H.; Wang, X.; Atia-Tul-Noor, A.; Wallace, W. C.; Douguet, N.; Bray, A.; Ivanov, I.; Bartschat, K.; Kheifets, A.; Sang, R. T.; Litvinyuk, I. V. Attosecond angular streaking and tunnelling time in atomic hydrogen. *Nature* **2019**, *568*, 75–77.
- (10) Muller, H. G. Reconstruction of attosecond harmonic beating by interference of two-photon transitions. *Appl. Phys. B* **2002**, *74*, s17–s21.
- (11) Palatchi, C.; Dahlström, J. M.; Kheifets, A. S.; Ivanov, I. A.; Canaday, D. M.; Agostini, P.; DiMauro, L. F. Atomic delay in helium, neon, argon and krypton. *J. Phys. B: At., Mol. Opt. Phys.* **2014**, 47, 245003.
- (12) Isinger, M.; Busto, D.; Mikaelsson, S.; Zhong, S.; Guo, C.; Salières, P.; Arnold, C. L.; L'Huillier, A.; Gisselbrecht, M. Accuracy and precision of the RABBIT technique. *Philos. Trans. R. Soc., A* **2019**, 377, 20170475.
- (13) Dahlström, J. M.; L'Huillier, A.; Maquet, A. Introduction to attosecond delays in photoionization. *J. Phys. B: At., Mol. Opt. Phys.* **2012**, 45, 183001.
- (14) Dahlström, J. M.; Guénot, D.; Klünder, K.; Gisselbrecht, M.; Mauritsson, J.; L'Huillier, A.; Maquet, A.; Taïeb, R. Theory of attosecond delays in laser-assisted photoionization. *Chem. Phys.* **2013**, 414, 53–64.
- (15) Baykusheva, D.; Wörner, H. J. Theory of attosecond delays in molecular photoionization. *J. chem. phys.* **2017**, *146*, 124306.
- (16) Pazourek, R.; Nagele, S.; Burgdörfer, J. Attosecond chronoscopy of photoemission. Rev. Mod. Phys. 2015, 87, 765.
- (17) Landsman, A. S.; Keller, U. Attosecond science and the tunnelling time problem. *Phys. Rep.* **2015**, 547, 1–24.
- (18) Ni, H.; Saalmann, U.; Rost, J.-M. Tunneling Ionization Time Resolved by Backpropagation. *Phys. Rev. Lett.* **2016**, *117*, No. 023002.
- (19) Vacher, M.; Steinberg, L.; Jenkins, A. J.; Bearpark, M. J.; Robb, M. A. Electron dynamics following photoionization: Decoherence due to the nuclear-wave-packet width. *Phys. Rev. A* **2015**, *92*, No. 040502.
- (20) Wigner, E. P. Lower limit for the energy derivative of the scattering phase shift. *Phys. Rev.* **1955**, 98, 145.
- (21) Smith, F. T. Lifetime matrix in collision theory. *Phys. RevPhysical Review* **1960**, *118*, 349.
- (22) Carroll, F. A. Perspectives on Structure and Mechanism in Organic Chemistry; 2nd Edition, Wiley: 2010.
- (23) Galasso, V. Photoionization cross-sections in ethylene: calculations by RPA and stieltjes imaging procedures. *J. Mol. Struct.:* THEOCHEM 1988, 168, 161–167.
- (24) Grimm, F. A.; Whitley, T. A.; Keller, P. R.; Taylor, J. W. Absolute partial photoionization cross sections of ethylene. *Chem. Phys.* **1991**, *154*, 303–309.
- (25) Brennan, J. G.; Cooper, G.; Green, J. C.; Payne, M. P.; Redfern, C. M. Relative partial photoionization cross-sections and photoelectron branching ratios of ethylene. *J. Electron Spectrosc. Relat. Phenom.* 1987, 43, 297–305.

(26) Frisch, M. J.; et al.. *Gaussian09*; Revision E.01. Gaussian Inc.: Wallingford CT 2009.

Supplementary Materials: The photo-ionization time in π -conjugated molecular systems

Deep Mukherjee, ¹ Shaul Mukamel, ² and Upendra Harbola ^{1, a)}

Here we present some essential ingredients used in the main text to compute the Wigner ionization time in Eq. (5). We first consider molecular orbitals for non-interacting case by linear combinations of atomic orbitals as ansatz. Using these orbitals, we then construct two-electron basis set to diagonalize the full interacting Hamiltonian to find its eigenstates and energies. We construct the scattering states as anti-symmetrized direct product of single electron cationic orbitals and the free electron orbitals. Thereafter, we compute transition dipole moments between the bound and the scattering states which is used to obtain the electron wave-packet in Eq. (4) in the main text. The derivative of phase of the wave-packet with respect to kinetic energy yields Wigner time(t_w) as given in Eq. (5) of the main text.

¹⁾Department of Inorganic and Physical Chemistry, Indian Institute of Science, Bangalore 560012, India

²⁾Department of Chemistry and Physics and Astronomy, University of California at Irvine, Irvine, CA, USA

a)Electronic mail: uharbola@iisc.ac.in

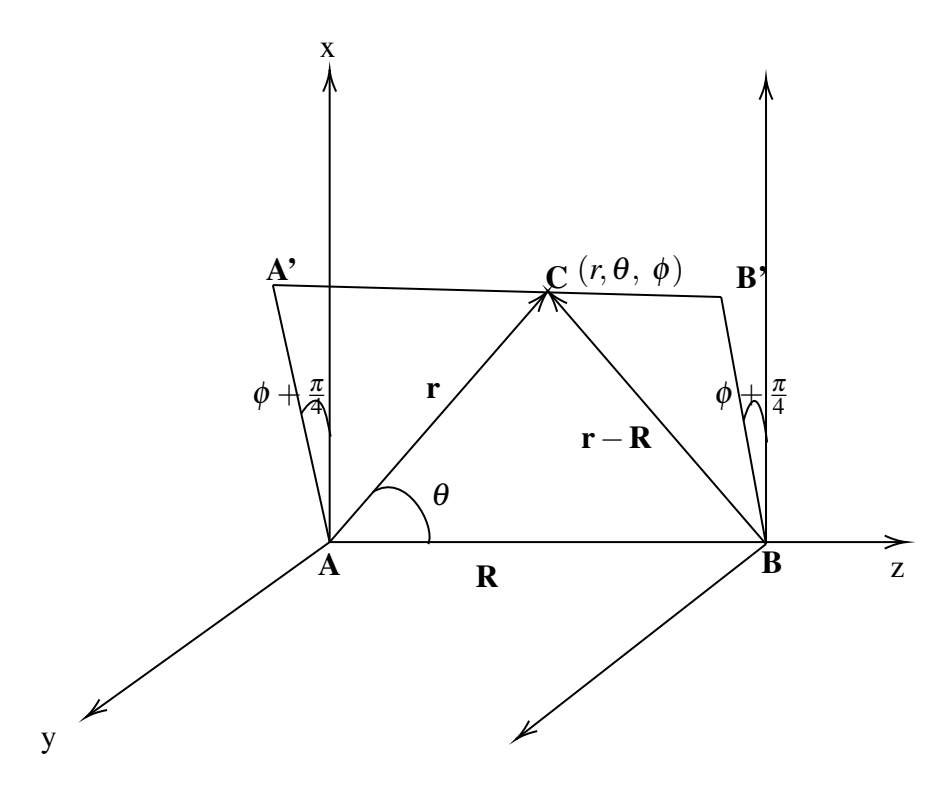


FIG. 1: Schematic diagram of two nuclei located along the \hat{z} -axis at points A and B. A is located at the origin. An electron is located at point C with coordinates (r, θ, ϕ) . \vec{AC} and \vec{BC} are in plane AA'B'B which makes angle $\theta + \frac{\pi}{4}$ from x - z plane.

We consider the coordinate system defined by two nuclei and one electron as depicted in Fig. (1).

CONSTRUCTION OF MOLECULAR ORBITALS

The π -type valence molecular orbitals which construct the two electron non-interacting states are formed by linear combinations of $2p_1$ type atomic orbitals centered on two different carbon atoms. These molecular orbitals are given as follows,

$$\phi_{H/L}(\mathbf{r}) = \frac{\psi_A(\mathbf{r}) \pm \psi_B(\mathbf{r})}{\sqrt{2(1 \pm S(R))}}$$
(1)

The atomic orbitals are given by,

$$\psi_{A} = \psi_{211}^{A}(r,\theta,\phi) = -\frac{1}{8\sqrt{\pi}} \left(\frac{z^{*}}{a}\right)^{\frac{3}{2}} \left(\frac{z^{*}r}{a}\right) e^{-\frac{z^{*}r}{2a}} \sin(\theta) e^{i\phi}. \tag{2}$$

$$\psi_{B} = \psi_{211}^{B}(r,\theta,\phi) = -\frac{1}{8\sqrt{\pi}} \left(\frac{z^{*}}{a}\right)^{\frac{3}{2}} \left(\frac{z^{*}r}{a}\right) e^{-\frac{z^{*}\sqrt{r^{2} + R^{2} - 2rR\cos(\theta)}}{2a}} \sin(\theta) e^{i\phi}. \tag{3}$$

Here ψ_{nlm}^X are Hydrogen-like atomic orbitals centered on atom X, with n, l, m being corresponding principal, azimuthal and magnetic quantum numbers and z^* is the effective nuclear charge due to the screening effects of the core electrons. R is the distance between two atoms and $a = \frac{4\pi\varepsilon_0\hbar^2}{me^2}$ is the bohr radius. The spatial overlap(S(R)) between ψ_A and ψ_B is obtained as follows,

$$S(R,b) = \frac{b^5}{2\pi} \int dr r^4 e^{-br} \int d\Omega \sin^2(\theta) e^{-b\sqrt{r^2 + R^2 - 2rR\cos(\theta)}},$$
 (4a)

where, $b=rac{z^*}{2a}$ and $d\Omega=\sin(\theta)d\theta d\phi$. Putting $\cos(\theta)=x$ we get,

$$S(R,b) = b^5 \int dr r^4 e^{-br} \int_{-1}^1 dx (1-x^2) e^{-b\sqrt{r^2+R^2-2rRx}}.$$
 (4b)

Let us consider the integral,

$$I = \int_{-1}^{1} dx (1 - x^2) e^{-a\sqrt{r^2 + R^2 - 2rRx}}.$$
 (4c)

Putting $u^2 = r^2 + R^2 - 2rRx$ and $udu = -\frac{1}{rR}dx$,

$$I = \frac{1}{4(rR)^3} \int_{r+R}^{|r-R|} du \left(u^5 - 2(r^2 + R^2)u^3 + (r^2 - R^2)^2 u \right) e^{-au}. \tag{4d}$$

By Substituting Eq. (4d) to Eq. (4b) and integrating over r we get,

$$S(R,b) = \frac{e^{-bR}}{15} \left(R^3 b^3 + 6R^2 b^2 + 15Rb + 15 \right). \tag{4e}$$

The two cationic molecular orbitals are similarly obtained as,

$$\phi_{H/L}^{C}(\mathbf{r}) = \frac{1}{\sqrt{2\left(1 \pm S(R, b')\right)}} \left(\psi_{A}^{cat}(\mathbf{r}) \pm \psi_{B}^{cat}(\mathbf{r})\right),\tag{5}$$

where +/- represents ground(H) / excited(L) cationic molecular orbital. ψ_A^{cat} and ψ_B^{cat} are cationic atomic orbitals obtained from Eq.(2) and Eq. (3) by replacing b with b'(>b).

To describe the ionized electron, the free electron basis orthogonal to bound orbital of the neutral system is chosen. This allows to maintain the orthogonality criterion between the bound and the scattering states of the molecular system. These are denoted as scattering orbital. The scattering orbital, $\phi_k(\mathbf{r})$, is orthogonal to neutral molecular orbitals^{1,2} and is given by,

$$\phi_k(\mathbf{r}) = \frac{e^{i\mathbf{k}\cdot\mathbf{r}}}{(2\pi)^{\frac{3}{2}}} - c_H(\mathbf{k})\phi_H(\mathbf{r}) - c_L(\mathbf{k})\phi_L(\mathbf{r}), \tag{6}$$

where coefficient $c_{H/L}(\mathbf{k})$ are given in Eqs.(61) and (62). The index 'k' on ϕ_k represents momentum of the electron in $\phi_k(\mathbf{r})$ state. Here c_H and c_L contain the effect of molecular potential on the free electron state. Note that due to contribution from molecular orbitals, $\phi_k(\mathbf{r})$ is not a definite momentum state. However, the molecular contribution decays quickly with increasing k value and $\phi_k(\mathbf{r})$ becomes effectively a free electron state with momentum \mathbf{k} .

The non-interacting two-electron basis to describe the bound states are constructed from the molecular orbitals $(\phi_{H/L}(\mathbf{r}))$ are given as,

$$\Phi^{0}(\mathbf{r}_{1},\mathbf{r}_{2}) = \phi_{H}(\mathbf{r}_{1})\phi_{H}(\mathbf{r}_{2}) \tag{7a}$$

$$\Phi_1^0(\mathbf{r_1}, \mathbf{r_2}) = \frac{1}{\sqrt{2}} \left[\phi_H(\mathbf{r_1}) \phi_L(\mathbf{r_2}) - \phi_L(\mathbf{r_1}) \phi_H(\mathbf{r_2}) \right]$$
(7b)

$$\Phi_2^0(\mathbf{r_1}, \mathbf{r_2}) = \phi_L(\mathbf{r_1})\phi_L(\mathbf{r_2}). \tag{7c}$$

Here only the state with zero spin is considered because in the electric pulse mediated ionization process spin is preserved. Since without any external interaction with light pulse ionization process is prohibited the scattering many-electron states must be orthogonal with respect to the neutral molecular states. This criterion is taken care by suitable choice of scattering orbitals as discussed above. These scattering states are formed as anti-symmetrized direct products of cation states and a single-electron scattering orbital, $\phi_k(\mathbf{r})$.

$$\Phi_{H/L,k}(\mathbf{r_1},\mathbf{r_2}) = \mathscr{\hat{A}}[\phi_{H/L}^C \otimes \phi_k]. \tag{8}$$

Here, $\hat{\mathscr{A}}$ is the anti-symmetric operator.

DIAGONALIZATION OF THE MOLECULAR HAMILTONIAN

There are three bound states of molecular Hamiltonian (H_M) which can be expressed in non-interacting two-electron basis. H_M can be written in terms of the non-interacting two-electron basis in Eq. (7) as follows:

$$H_{M} = \begin{bmatrix} H_{11} & H_{12} & H_{13} \\ H_{12} & H_{22} & H_{23} \\ H_{13} & H_{23} & H_{33}. \end{bmatrix}$$
(9)

Matrix elements H_{ij} , i, j = 1, 2, 3 are given below in Eqs. (21)-(25).

Eigenvalues and eigenvectors of the full molecular Hamiltonian are obtained by diagonalizing H_M . The eigenvalues are given by,

$$E_0 = \frac{H_{11} + H_{33} - \sqrt{(H_{11} - H_{33})^2 + 4H_{13}^2}}{2}$$
 (10a)

$$E_1 = H_{22} (10b)$$

$$E_2 = \frac{H_{11} + H_{33} + \sqrt{(H_{11} - H_{33})^2 + 4H_{13}^2}}{2}.$$
 (10c)

The respective eigenstates are written as,

$$\Phi(\mathbf{r_1}, \mathbf{r_2}) = \frac{(E_0 - H_{33})\Phi^0(\mathbf{r_1}, \mathbf{r_2}) + H_{13}\Phi_2^0(\mathbf{r_1}, \mathbf{r_2})}{\sqrt{(E_0 - H_{33})^2 + H_{13}^2}}$$
(11a)

$$\Phi_1(\mathbf{r_1}, \mathbf{r_2}) = \Phi_1^0(\mathbf{r_1}, \mathbf{r_2}) \tag{11b}$$

$$\Phi_2(\mathbf{r_1}, \mathbf{r_2}) = \frac{(E_0 - H_{33})\Phi^0(\mathbf{r_1}, \mathbf{r_2}) - H_{13}\Phi^0_2(\mathbf{r_1}, \mathbf{r_2})}{\sqrt{(E_0 - H_{33})^2 + H_{13}^2}}$$
(11c)

CALCULATION OF THE HAMILTONIAN MATRIX ELEMENTS

The following integrals are important to calculate the matrix elements of the full Hamiltonian,

$$E(b) = \int d^3 \mathbf{r} \psi_A^*(\mathbf{r}) \left[-\frac{1}{2} \nabla^2 - \frac{z^*}{r} \right] \psi_A(\mathbf{r}) = -a^2 b^2 E'.$$
 (12)

E' is the ground state ionization energy of Hydrogen atom.

$$\tilde{\alpha}(R,b) = \int d^{3}\mathbf{r}\psi_{A}^{*}(\mathbf{r}) \frac{z^{*}}{|\mathbf{r} - \mathbf{R}|} \psi_{A}(\mathbf{r})$$

$$= \frac{1}{bR^{3}} \left[e^{-2bR} \left(3 + 6bR + 4b^{2}R^{2} + b^{3}R^{3} \right) - (3 - 2b^{2}R^{2}) \right], \qquad (13)$$

$$\tilde{\beta}(R,b) = \int d^{3}\mathbf{r}\psi_{A}^{*}(\mathbf{r}) \frac{z^{*}}{r} \psi_{B}(\mathbf{r})$$

$$= \frac{b^{2}e^{-bR}}{3} \left(3 + 3bR + b^{2}R^{2} \right). \qquad (14)$$

The two-electron integrals are then calculated by expressing two-electron repulsion potential in terms of infinite sum of Legendre polynomial(P_l) as follows:

$$\frac{1}{|\mathbf{r}_1 - \mathbf{r}_2|} = \sum_{l} \frac{r_{<}^{l}}{r_{>}^{l+1}} P_l(\cos(\theta')). \tag{15}$$

 $r_{<}(r_{>})$ is denoted as the lesser(greater) among $\mathbf{r_{1}}$ and $\mathbf{r_{2}}$. The angle between $\mathbf{r_{1}}$ and $\mathbf{r_{2}}$ is θ' . $P_{l}(\cos(\theta))$ is written in terms of the product of spherical harmonics $Y_{l,m}(\theta,\phi)$ as follows,

$$P_{l}(\cos(\theta)) = \frac{4\pi}{2l+1} \sum_{m=-l}^{l} Y_{l,m}(\theta_{1}, \phi_{1}) Y_{l,m}^{*}(\theta_{2}, \phi_{2}).$$
(16)

$$J_{2} = \int d^{3}\mathbf{r}_{1}d^{3}\mathbf{r}_{2}\psi_{A}^{*}(\mathbf{r}_{1})\psi_{A}^{*}(\mathbf{r}_{2})\frac{1}{|\mathbf{r}_{1}-\mathbf{r}_{2}|}\psi_{A}(\mathbf{r}_{1})\psi_{A}(\mathbf{r}_{2})$$

$$= \frac{237}{640}b.$$

$$J_{1} = \int d^{3}\mathbf{r}_{1}d^{3}\mathbf{r}_{2}\psi_{A}^{*}(\mathbf{r}_{1})\psi_{B}^{*}(\mathbf{r}_{2})\frac{1}{|\mathbf{r}_{1}-\mathbf{r}_{2}|}\psi_{A}(\mathbf{r}_{1})\psi_{A}(\mathbf{r}_{2})$$

$$= e^{-3bR} \left[\frac{693}{512} + \frac{2079}{512}bR + \frac{107}{32}b^{2}R^{2} + \frac{41}{32}b^{3}R^{3} + \frac{1}{4}b^{4}R^{4} + \frac{1}{48}b^{5}R^{5}\right]$$

$$+ e^{-bR} \left[-\frac{693}{512} - \frac{693}{512}bR + \frac{265}{128}b^{2}R^{2} - \frac{35}{64}b^{3}R^{3} + \frac{1}{2}b^{4}R^{4} + \frac{1}{6}b^{5}R^{5}\right].$$
(18)

We have taken only the contribution for P_0 , as the the contribution for P_2 is extremely small compared to that of P_0 .

$$J_{0} = \int d^{3}\mathbf{r}_{1}d^{3}\mathbf{r}_{2}\psi_{A}^{*}(\mathbf{r}_{1})\psi_{B}^{*}(\mathbf{r}_{2})\frac{1}{|\mathbf{r}_{1}-\mathbf{r}_{2}|}\psi_{B}(\mathbf{r}_{1})\psi_{A}(\mathbf{r}_{2})$$

$$= e^{-4bR} \left[\frac{6435}{512} + \frac{6435}{128}bR + \frac{34749}{512}b^{2}R^{2} + \frac{5709}{128}b^{3}R^{3} + \frac{1023}{64}b^{4}R^{4} + \frac{49}{16}b^{5}R^{5} + \frac{1}{4}b^{6}R^{6} \right]$$

$$+ e^{-2bR} \left[-\frac{6435}{512} - \frac{6435}{256}bR + \frac{3861}{512}b^{2}R^{2} + \frac{1881}{256}b^{3}R^{3} - \frac{495}{128}b^{4}R^{4} + \frac{1}{32}b^{5}R^{5} + \frac{25}{32}b^{6}R^{6} + \frac{22}{35}b^{7}R^{7} + \frac{131}{210}b^{8}R^{8} + \frac{101}{315}b^{9}R^{9} + \frac{5}{63}b^{10}R^{10} + \frac{5}{630}b^{11}R^{11} \right].$$

$$(19)$$

$$\rho_{0} = \int d^{3}\mathbf{r}_{1}d^{3}\mathbf{r}_{2}\psi_{A}^{*}(\mathbf{r}_{1})\psi_{A}^{*}(\mathbf{r}_{2})\frac{1}{|\mathbf{r}_{1} - \mathbf{r}_{2}|}\psi_{B}(\mathbf{r}_{1})\psi_{B}(\mathbf{r}_{2})$$

$$= \frac{e^{-2bR}}{b^{2}R^{3}}\left(\frac{3}{2} + 3(bR) + 2(bR)^{2} + \frac{93}{256}(bR)^{3} - \frac{35}{128}(bR)^{4} - \frac{71}{320}(bR)^{5} - \frac{19}{240}(bR)^{6} - \frac{9}{560}(bR)^{7} + \frac{1}{630}(bR)^{8}\right) - \frac{1}{2}\left(\frac{3}{b^{2}R^{3}} - \frac{2}{R}\right). \tag{20}$$

We can write the matrix elements in terms of the above expressions as follows,

$$H_{11} = \int d^{3}\mathbf{r}_{1} \int d^{3}\mathbf{r}_{2} \Phi^{0*}(\mathbf{r}_{1}, \mathbf{r}_{2}) \hat{H} \Phi^{0}(\mathbf{r}_{1}, \mathbf{r}_{2})$$

$$= 2E - 2\left(\frac{\tilde{\alpha}(R, b) + \tilde{\beta}(R, b)}{1 + S(R, b)}\right) + \frac{J_{2} + 4J_{1} + 2J_{0} + \rho_{0}}{2(1 + S(R, b))^{2}}, \qquad (21)$$

$$H_{22} = \int d^{3}\mathbf{r}_{1} \int d^{3}\mathbf{r}_{2} \Phi_{1}^{0*}(\mathbf{r}_{1}, \mathbf{r}_{2}) \hat{H} \Phi_{1}^{0}(\mathbf{r}_{1}, \mathbf{r}_{2})$$

$$= 2E - 2\left(\frac{\tilde{\alpha}(R, b) - S(R, b)\tilde{\beta}(R, b)}{1 - S^{2}(R, b)}\right) + \left(\frac{\rho_{0} - J_{0}}{1 - S^{2}}\right), \qquad (22)$$

$$H_{33} = \int d^{3}\mathbf{r}_{1} \int d^{3}\mathbf{r}_{2} \Phi_{2}^{0*}(\mathbf{r}_{1}, \mathbf{r}_{2}) \hat{H} \Phi_{2}^{0}(\mathbf{r}_{1}, \mathbf{r}_{2})$$

$$= 2E - 2\left(\frac{\tilde{\alpha}(R, b) - \tilde{\beta}(R, b)}{1 - S(R, b)}\right) + \frac{J_{2} - 4J_{1} + 2J_{0} + \rho_{0}}{2(1 - S(R, b))^{2}}, \qquad (23)$$

and,

$$H_{12} = H_{21} = H_{23} = H_{32} = 0. (24)$$

$$H_{31} = H_{13} = \frac{J_2 - \rho_0}{2(1 - S^2(R, b))}. (25)$$

The energy $E_{H/L}$ for single particle cationic orbital is given as,

$$E_{H/L} = E(b') - \left(\frac{\tilde{\alpha}(R,b') \pm \tilde{\beta}(R,b')}{1 \pm S(R,b')}\right). \tag{26}$$

Parameters obtained from quantum chemistry

To obtain the effective nuclear charge (z^*) for the neutral and the cation molecule, we perform Density Functional Theory calculation. We use b3lyp functional and 6-31g(d,p) basis to obtain energy differences between neutral and cationic state as a function of C-C bond. We then fit this data with the theoretical function $E_0 - E_H$ (Eqs. 10a and 26 in SM) around the equilibrium R = 2.19 au by varying z^* for neutral and cationic systems. This gives $z^* = 1.8$ au for the neutral and $z^* = 2.2$ au for the cationic system. The force constant κ and V are obtained by fitting the DFT data for the total energy of ethylene molecule around the equilibrium with the potential energy function in Eq. (2) in the main text. This gives $\kappa = 1.38$ au and V = ... au.

DIPOLE MATRIX ELEMENTS

Dipole matrix element between scattering state and the bound state:

The matrix element of the dipole operator between the scattering state $\Phi_{I,k}(\mathbf{r}_1,\mathbf{r})$ and the neutral ground molecular state $\Phi(\mathbf{r}_1,\mathbf{r})$ is given as,

$$\mu_I(\mathbf{k}) = \int d^3 \mathbf{r}_1 \int d^3 \mathbf{r} \Phi_{I,k}^*(\mathbf{r}_1, \mathbf{r}) \hat{\mathbf{r}} \Phi(\mathbf{r}_1, \mathbf{r}). \tag{27}$$

Note that 'r' is the vector coordinate for the ionized electron.

The dipole matrix element (Eq. (27)) is computed using Dyson orbitals³ in the following way,

$$\mu_{I}(\mathbf{k}) = \int d^{3}\mathbf{r}_{1}d^{3}\mathbf{r}\Phi_{I,k}^{*}(\mathbf{r}_{1},\mathbf{r})\hat{\mathbf{r}}\Phi(\mathbf{r}_{1},\mathbf{r}) + \Phi_{I,k}^{*}(\mathbf{r}_{1},\mathbf{r})\hat{\mathbf{r}}_{1}\Phi(\mathbf{r}_{1},\mathbf{r}),$$

$$= \int d^{3}\mathbf{r}\phi_{k}^{*}(\mathbf{r})\mathbf{r} \int d^{3}\mathbf{r}_{1}\phi_{I}^{C*}(\mathbf{r}_{1})\Phi(\mathbf{r}_{1},\mathbf{r}) + \int d^{3}\mathbf{r}\phi_{k}(\mathbf{r}) \int d^{3}\mathbf{r}_{1}\phi_{I}^{C*}(\mathbf{r}_{1})\mathbf{r}\Phi(\mathbf{r},\mathbf{r}_{1}),$$

$$= \int d^{3}\mathbf{r}\phi_{k}^{*}(\mathbf{r})\mathbf{r}\mathcal{D}_{I}(\mathbf{r}) + \int d^{3}\mathbf{r}_{1}\mathbf{r}_{1}\phi_{I}^{C*}(\mathbf{r}_{1}) \int d^{3}\mathbf{r}\phi_{k}^{*}(\mathbf{r})\Phi(\mathbf{r},\mathbf{r}_{1}). \tag{28}$$

 $\mathscr{D}_I(\mathbf{r}) = \int d^3\mathbf{r_1}\phi_I^{C*}(\mathbf{r_1})\Phi(\mathbf{r_1},\mathbf{r})$ is Dyson orbital corresponding to the I'th cationic and the neutral ground states. $\mathscr{D}_I(\mathbf{r})$ may be interpreted as the electron wave-packet corresponding to the elec-

tron being ionized keeping the cationic system in the I'th state. Since the scattered orbitals are orthogonal to neutral orbitals, the second term in the above equation becomes zero. Hence, $\mu_I(\mathbf{k})$ is written as,

$$\mu_{I}(\mathbf{k}) = \int d^{3}\mathbf{r}\phi_{k}^{*}(\mathbf{r})\mathbf{r}\mathcal{D}_{I}(\mathbf{r})$$

$$= \int d^{3}\mathbf{r} \left[\frac{e^{-i\mathbf{k}\cdot\mathbf{r}}}{(2\pi)^{3/2}} - c_{H}^{*}(\mathbf{k})\phi_{H}^{*}(\mathbf{r}) - c_{L}^{*}(\mathbf{k})\phi_{L}^{*}(\mathbf{r}) \right] \mathbf{r}\mathcal{D}_{I}(\mathbf{r})$$
(29)

The Dyson orbitals $(\mathcal{D}_I(\mathbf{r}))$ mentioned above are given as follows:

$$\mathcal{D}_H(\mathbf{r}) = D_H(R)\phi_H(\mathbf{r}),\tag{30}$$

$$\mathscr{D}_L(\mathbf{r}) = D_L(R)\phi_L(\mathbf{r}),\tag{31}$$

where $D_{H/L}(R)$ are the Dyson orbital coefficient given as,

$$D_H(R) = \frac{E_0 - H_{33}}{N\sqrt{(1 + S(R,b))(1 + S(R,b'))}} \left[\left(\frac{2\sqrt{bb'}}{b + b'} \right)^5 + S(R,b,b') \right]$$
(32)

$$D_L(R) = \frac{H_{13}}{N\sqrt{(1 - S(R,b))(1 - S(R,b'))}} \left[\left(\frac{2\sqrt{bb'}}{b + b'} \right)^5 - S(R,b,b') \right], \tag{33}$$

where, $b' = \frac{z'}{2a}$.

$$S(R,b,b') = \frac{(bb')^{5/2}}{(b^2 - b'^2)^5 R^3} e^{-(b+b')R} \Big(32be^{bR} \Big(R^3 (b^2 - b'^2)^2 + 12b'R^2 (b' - b)(b+b') + 48b'^2 R + 48b' \Big) - 32b'e^{b'R} \Big(R^3 (b^2 - b'^2)^2 + 48b^2 R + 12bR^2 (b - b')(b+b') + 48b \Big) \Big),$$
(34)

$$N = \sqrt{(E_0 - H_{33})^2 + H_{13}^2}. (35)$$

Substituting for the Dyson orbitals in Eq. (29), we note that calculation of $\mu_I(\mathbf{k})$ requires dipole elements between molecular bound orbitals and the free particle wave-function, $\phi(k)$. This is calculated as follows.

$$\mu_{H/L} = \int d^{3}\mathbf{r}e^{-ik.r}(r_{x}\hat{x} + r_{y}\hat{y} + r_{z}\hat{z})\phi_{H/L}(\mathbf{r})$$

$$= \sum_{i=x,y,z} \hat{i} \frac{\mu_{i}^{A} \pm \mu_{i}^{B}}{\sqrt{2(1 \pm S(R))}}$$
(36)

 $\mu_i^{A/B}$ is defined as,

$$\mu_{i}^{A/B} = \int d^{3}r e^{-ik.r} (r_{x}\hat{x} + r_{y}\hat{y} + r_{z}\hat{z}) \psi_{A/B}$$

$$= \int d^{3}r e^{-i(k_{x}r_{x} + k_{y}r_{y} + k_{z}r_{z})} (r_{x}\hat{x} + r_{y}\hat{y} + r_{z}\hat{z}) \psi_{A/B}$$

$$= i \frac{\partial}{\partial k_{i}} \int d^{3}r e^{-i(k_{x}r_{x} + k_{y}r_{y} + k_{z}r_{z})} \psi_{A/B}$$

$$= i \frac{\partial}{\partial k_{i}} c *_{A/B} (k, \vartheta, \varphi)$$
(37)

We can write the derivative operator $\frac{\partial}{\partial k_i}$ in terms of k, ϑ and φ as follows:

$$\frac{\partial}{\partial k_z} = \cos(\vartheta) \frac{\partial}{\partial k} - \frac{\sin(\vartheta)}{k} \frac{\partial}{\partial \vartheta}$$
(38)

$$\frac{\partial}{\partial k_x} = \sin(\vartheta)\cos(\varphi)\frac{\partial}{\partial k} + \frac{\cos(\vartheta)\cos(\varphi)}{k}\frac{\partial}{\partial \vartheta} - \frac{\sin(\varphi)}{k\sin(\vartheta)}\frac{\partial}{\partial \varphi}$$
(39)

$$\frac{\partial}{\partial k_{y}} = \sin(\vartheta)\sin(\varphi)\frac{\partial}{\partial k} + \frac{\cos(\vartheta)\sin(\varphi)}{k}\frac{\partial}{\partial \vartheta} + \frac{\cos(\varphi)}{k\sin(\vartheta)}\frac{\partial}{\partial \varphi}$$
(40)

We obtain $\mu_z^{A/B}$ as follows,

$$\mu_{z}^{A} = -\frac{24b^{7/2}e^{i\varphi}k^{2}\sin(2\vartheta)}{\pi(b^{2}+k^{2})^{4}}$$

$$= -\frac{48b^{7/2}}{\pi(b^{2}+k^{2})^{4}}\left(k_{z}(k_{x}+ik_{y})\right)$$

$$\mu_{z}^{B} = \frac{8b^{7/2}e^{i\varphi}}{\pi(b^{2}+k^{2})^{3}}\left(ikR\sin(\vartheta) + 3\sin(2\vartheta)\frac{k^{2}}{b^{2}+k^{2}}\right)\exp(-ikR\cos(\vartheta))$$

$$= \frac{8b^{7/2}}{\pi(b^{2}+k^{2})^{3}}\left(i(k_{x}+ik_{y})R + \frac{6k_{z}(k_{x}+ik_{y})}{b^{2}+k^{2}}\right)e^{-ik_{z}R}$$
(42)

 $\mu_x^{A/B}$ are obtained as,

$$\mu_{x}^{A} = \frac{8b^{7/2}}{\pi(b^{2} + k^{2})^{3}} \left(1 - 6e^{i\varphi} \sin^{2}(\vartheta) \cos(\varphi) \frac{k^{2}}{b^{2} + k^{2}} \right)$$

$$= \frac{8b^{7/2}}{\pi(b^{2} + k^{2})^{3}} \left(1 - 6\frac{k_{x}(k_{x} + ik_{y})}{b^{2} + k^{2}} \right)$$

$$\mu_{x}^{B} = \left(\frac{8b^{7/2}}{\pi(b^{2} + k^{2})^{3}} \left(1 - 6e^{i\varphi} \sin^{2}(\vartheta) \cos(\varphi) \frac{k^{2}}{b^{2} + k^{2}} \right) \right) \exp(-ikR\cos(\vartheta))$$

$$= \frac{8b^{7/2}}{\pi(b^{2} + k^{2})^{3}} \left(1 - 6\frac{k_{x}(k_{x} + ik_{y})}{b^{2} + k^{2}} \right) e^{-ik_{z}R}$$
(44)

 $\mu_{y}^{A/B}$ are obtained as,

$$\mu_{y}^{A} = i \frac{8b^{7/2}}{\pi (b^{2} + k^{2})^{3}} \left(1 + i6e^{i\varphi} \sin^{2}(\vartheta) \sin(\varphi) \frac{k^{2}}{b^{2} + k^{2}} \right)$$

$$= i \frac{8b^{7/2}}{\pi (b^{2} + k^{2})^{3}} \left(1 + i6\frac{k_{y}(k_{x} + ik_{y})}{b^{2} + k^{2}} \right)$$

$$\mu_{y}^{B} = \frac{8b^{7/2}}{\pi (b^{2} + k^{2})^{3}} \left(1 + i6e^{i\varphi} \sin^{2}(\vartheta) \sin(\varphi) \frac{k^{2}}{b^{2} + k^{2}} \right) \exp(-ikR\cos(\vartheta))$$

$$= i \frac{8b^{7/2}}{\pi (b^{2} + k^{2})^{3}} \left(1 + i6\frac{k_{y}(k_{x} + ik_{y})}{b^{2} + k^{2}} \right) e^{-ik_{z}R}.$$
(46)

The x, y and z component of $\mu_I(\mathbf{k})(I = H, L)$ are given as follows

$$\hat{x} \cdot \mu_{H/L}(\mathbf{k}) = \frac{24\sqrt{2}D_{H/L}(R)}{\sqrt{1 \pm S(R)}} \frac{b^{7/2}}{\pi (b^2 + k^2)^3} \left(\frac{k_x(k_x + ik_y)}{b^2 + k^2} - \frac{1}{6}\right) \left(1 \pm e^{-ik_z R}\right)$$
(47)

$$\hat{\mathbf{y}} \cdot \mu_{H/L}(\mathbf{k}) = \frac{24\sqrt{2}D_{H/L}(R)}{\sqrt{1 \pm S(R)}} \frac{b^{7/2}}{\pi (b^2 + k^2)^3} \left(\frac{k_y(k_x + ik_y)}{b^2 + k^2} - \frac{i}{6}\right) \left(1 \pm e^{-ik_z R}\right),\tag{48}$$

$$\hat{z} \cdot \mu_{H/L}(\mathbf{k}) = D_{H/L}(R) \left[\frac{1}{\sqrt{2(1 \pm S(R))}} \frac{8b^{7/2}(k_x + ik_y)}{\pi (b^2 + k^2)^3} \left[\frac{6k_z}{b^2 + k^2} (1 \pm e^{-ik_z R}) \pm iRe^{-ik_z R} \right] - \frac{c_{H/L}^*(\mathbf{k})RS(R)}{2(1 \pm S(R))} \right]$$
(49)

where the parameter $b(=\frac{z}{2a}, a)$ is the bohr radius) represents the effective nuclear charge as felt by the π -electrons. S is the overlap between atomic orbitals given in Eq.(4) and $D_{H/L}(R)$ are defined in Eqs.(32) and (33).

Dipole matrix element between bound states:

The dipole moment between bound orbitals are given by,

$$\int d^3 \mathbf{r} \phi_X^*(\mathbf{r}) (r_x \hat{x} + r_y \hat{y} + r_z \hat{z}) \phi_Y(\mathbf{r}), \tag{50}$$

where i = x, y, z three different components of dipole moment along the respective directions. X, Y denote the molecular orbitals H and L. The dipole moment between atomic orbitals centered at same coordinate becomes zero, which is evident from symmetry argument. When the two orbital orbitals are centered on two different coordinate the dipole moment matrix element obtained as

follows,

$$\frac{e^{-bR}}{30}(b^3R^4 + 6b^2R^3 + 15bR^2 + 15R) = \frac{RS(R)}{2}.$$
 (51)

The dipole moment along x and y direction between the bound orbitals becomes zero.

Calculation of $c_{H/L}$

To construct the scattered orbital($\phi_k(r)$) orthogonal to neutral molecular orbital we calculate the overlap of molecular orbital with free particle wave function and subtract their contribution from the free particle wave function. c_H/c_L is the overlap of molecular bonding/anti-bonding orbital with free particle wave function. c_H/c_L is expressed in terms of atomic overlap integrals c_X (where X correspond to atomic center X = A, B)in the following way.

$$c_H(k, \vartheta, \varphi) = \frac{1}{\sqrt{2(1+S(R))}} \Big(c_A + c_B \Big), \tag{52}$$

$$c_L(k,\vartheta,\varphi) = \frac{1}{\sqrt{2(1-S(R))}} \Big(c_A - c_B \Big). \tag{53}$$

In order to compute c_X , we express $e^{ik.r}$ in spherical co-ordinate,

$$e^{i\mathbf{k}\cdot\mathbf{x}} = 4\pi \sum_{l=0}^{\infty} \sum_{m=-l}^{l} i^{l} j_{l}(kr) Y_{lm}(\theta, \phi) Y_{lm}^{*}(\vartheta, \phi).$$
 (54)

 $j_l(kr)$ is l'th spherical Bessel function. c_A is then calculated as,

$$\begin{split} c_A &= \frac{1}{(\sqrt{2\pi})^3} \int d^3r \psi_A^* e^{ik.r} \\ &= \sqrt{\frac{2}{\pi}} \sum_{l=0}^{\infty} \sum_{m=-l}^{l} i^l \int d^3r \psi_A^*(r,\theta,\phi) j_l(kr) Y_{lm}(\theta,\phi) Y_{lm}^*(\vartheta,\phi) \\ &= \frac{1}{4\sqrt{2\pi}} (\frac{z}{a})^{5/2} \sum_{l=0}^{\infty} \sum_{m=-l}^{l} i^l \int dr r^3 j_l(kr) e^{-\frac{zr}{2a}} \int d\theta d\phi \sin^2(\theta) e^{-i\phi} Y_{lm}(\theta,\phi) Y_{lm}^*(\vartheta,\phi). \end{split}$$

By applying the substitution $b = \frac{z}{2a}$, we get,

$$=\frac{b^{5/2}}{\pi}\sum_{l=0}^{\infty}\sum_{m=-l}^{l}i^{l}\int dr r^{3}j_{l}(kr)e^{-br}\int d\theta d\phi\sin^{2}(\theta)e^{-i\phi}Y_{lm}(\theta,\phi)Y_{lm}^{*}(\vartheta,\varphi). \tag{55a}$$

Integration over spherical coordinate gives,

$$c_A(k,\vartheta,\varphi) = \frac{8b^{7/2}e^{-i\varphi}k\sin(\vartheta)}{i\pi(b^2 + k^2)^3},$$
(55b)

where ψ^B is not centered at origin. We calculate the overlap for electronic wave-packet with ψ_B , c_B which is defined as,

$$c_B(\mathbf{k}) = \frac{1}{(2\pi)^{3/2}} \int d^3r \psi_B^*(r) e^{ik \cdot r}.$$
 (56)

From the Eq.(2) and Eq.(3) we can clearly see that, $\psi_B(\vec{r})$ can be expressed in terms of $\psi_A(\vec{r})$ as follows.

$$\psi_B(\vec{r}) = \psi_A(\vec{r} - \vec{R}). \tag{57}$$

Substituting the form of ψ_b in terms of ψ_A in the Eq.(56), we get,

$$c_B(\mathbf{k}) = \frac{1}{(2\pi)^{3/2}} \int d^3r \psi_B^*(r) e^{ik \cdot r}$$

$$= \frac{1}{(2\pi)^{3/2}} \int d^3r \psi_A^*(\vec{r} - \vec{R}) e^{ik \cdot r}.$$
(58)

Substituting, $\vec{z} = \vec{r} - \vec{R}$, in above equation we get,

$$c_B(k, \vartheta, \varphi) = \frac{e^{ik \cdot R}}{(2\pi)^{3/2}} \int dz^3 \psi_A^*(z) e^{ik \cdot z}$$
$$= e^{ikR\cos(\vartheta)} c_A(k, \vartheta, \varphi). \tag{60}$$

Hence, $c_{H/L}(\mathbf{k})$ is given as,

$$c_{H}(\mathbf{k}) = -\frac{8b^{7/2}}{\pi (b^{2} + k^{2})^{3} \sqrt{2(1 + S(R))}} (ik_{x} + k_{y}) \left[1 + e^{ik_{z}R}\right]$$

$$c_{L}(\mathbf{k}) = -\frac{8b^{7/2}}{\pi (b^{2} + k^{2})^{3} \sqrt{2(1 - S(R))}} (ik_{x} + k_{y}) \left[1 - e^{ik_{z}R}\right].$$
(62)

$$c_L(\mathbf{k}) = -\frac{8b^{7/2}}{\pi (b^2 + k^2)^3 \sqrt{2(1 - S(R))}} (ik_x + k_y) \left[1 - e^{ik_z R}\right]. \tag{62}$$

CALCULATION OF PHASE AND CORRESPONDING IONIZATION TIME:

Wigner ionization $timet_W(\mathbf{k}, R)$ is calculated from the energy derivative of the phase of freeelectron wave-packet. The phase of the wave-packet in Eq. (4) in the main text is given by,

$$\tan(\mathscr{P}) = \frac{u}{v},\tag{63}$$

Where,

$$u = u_H + \chi u_L, \tag{64}$$

$$v = v_H + \chi v_L. \tag{65}$$

 u_H , u_L , v_H , v_L are given by,

$$u_H = -m(1 + \cos(k_z R)) - R\sin(k_z R) + \frac{RS}{2(1+S)}\sin(k_z R)$$
(66)

$$u_L = -m(1 - \cos(k_z R)) - R\sin(k_z R) + \frac{RS}{2(1 - S)}\sin(k_z R), \tag{67}$$

$$v_H = -m(\sin(k_z R)) + R\cos(k_z R) - \frac{RS}{2(1+S)}(1+\cos(k_z R))$$
(68)

$$v_L = m(\sin(k_z R)) - R\cos(k_z R) - \frac{RS}{2(1-S)}\cos(k_z R).$$
(69)

Here,
$$m = \frac{6k_z}{b^2 + k^2}$$
 and $\chi = \sqrt{\frac{1+S}{1-S}} \frac{D_H(R)}{D_L(R)} \frac{e^{-\frac{(\omega_X - \frac{k^2}{2} + E_0 - E_L)^2}{4a}}}{e^{-\frac{(\omega_X - \frac{k^2}{2} + E_0 - E_H)^2}{4a}}}.$

Wigner ionization time($t_W(\mathbf{k}, R)$) is given as

$$t_W(\mathbf{k}, R) = \frac{1}{k} \frac{\partial \mathscr{P}}{\partial k}.$$
 (70)

This results in Eq. (5) of the main text.

WAVE-PACKET AND ANGLE RESOLVED t_W :

The Wigner ionization time, $t_W(\mathbf{k},R)$, calculated from Eq. (5) in the main text, is antisymmetric with respect to $\vartheta = \frac{\pi}{2}$ for all k, while ϑ -dependent photo-ionized electron probability density, $|\Psi_k(\vartheta)|^2$, is symmetric, as shown in Fig. (3). This symmetry in $t_W(\mathbf{k},R)$ and $|\Psi_k(\vartheta)|^2$

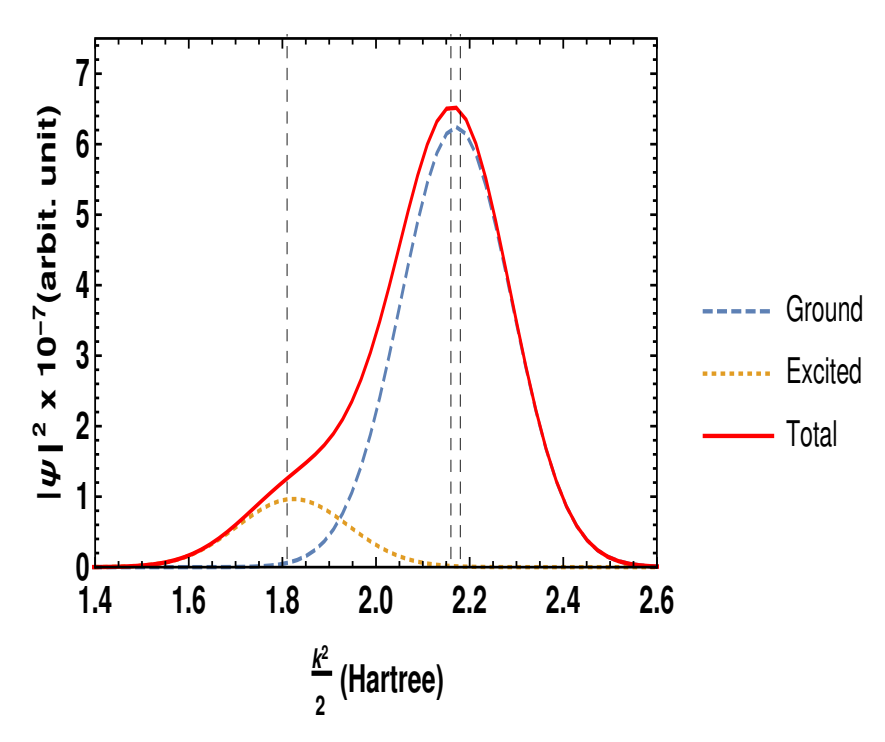


FIG. 2: Photo-electron spectrum (solid curve) for the ionization of the eth ylene model system by a 68 eV XUV pulse ($\mathcal{E}_0 = 0.01$ au and FWHM 242 as) at equilibrium R = 2.19 au. Dashed and dotted curves represent contributions to $|\Psi_k|^2$ coming from the ground and excited cationic states, respectively. The dashed vertical lines show the peak positions.

is due to the same symmetry of the ground neutral state. The negative values of $t_W(\mathbf{k}, R)$ suggests the peak of the XUV pulse recedes that of the photo-electron waver-packet. For instantaneous ionization for all \mathbf{k} , the two peaks must appear at zero time, when the XUV is maximum.

From the angular symmetry of $t_W(\mathbf{k},R)$ and $|\psi_k|^2$, we conclude that the electrons having positive and negative $t_W(\mathbf{k},R)$ are equally probable, that is, the intensity of the forward and the backward scattered electrons is the same. Note that in both directions, for a given kinetic energy of scattered electron, electrons having positive as well as negative $t_W(\mathbf{k},R)$ contribute to the same intensity.

DRESSED SCATTERING STATES IN STREAKING PROCESS

In case of the streaking experiment, we need to "dress" the scattering states with the IR vector potential as discussed in the main text. The effect of the IR field can be incorporated by modifying

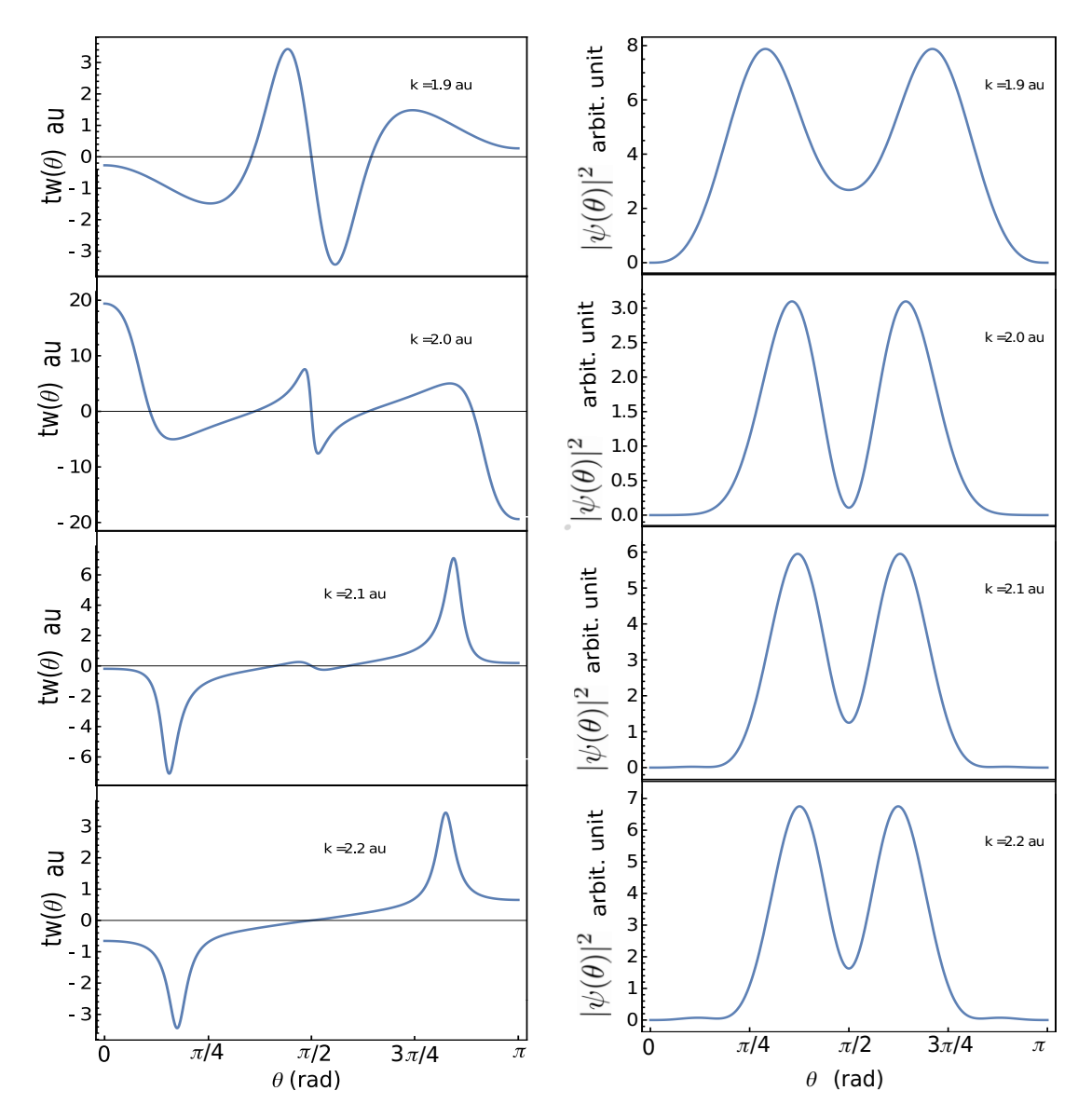


FIG. 3: Left panel: Wigner ionization time-delay($t_W(\mathbf{k}, R)$) for several values of k in atomic unit at equilibrium, R = 2.19 au. Right Panel: Ionization probability($|\Psi(k, \vartheta, R)|^2$) for corresponding k and R.

the scattering state, Eq.(6), due to the IR vector potential,

$$\phi_{\mathbf{k}}(\mathbf{r},t;t') = \frac{e^{i(\mathbf{k}'+\mathbf{A}(t)-\mathbf{A}(t'))\cdot\mathbf{r}}}{\sqrt{(2\pi)^3}} - c_H(\mathbf{k}',t,t')\phi_H(\mathbf{r}) - c_L(\mathbf{k}',t,t')\phi_L(\mathbf{r}).$$
(71)

Here $\mathbf{A}(t) - \mathbf{A}(t')$ represents change in momentum of the scattering wave-packet during the time t - t'. Note that the momentum $\mathbf{k}' (\equiv \mathbf{k}(t'))$ represents the kinetic momentum of the free electron at t'. The canonical momentum $\mathbf{p} = \mathbf{k}(t') - \mathbf{A}(t') = \mathbf{k}(t) - \mathbf{A}(t)$ remains constant. $\phi_{\mathbf{k}}(r,t,t')$ can

then be written in term of canonical momentum as,

$$\phi_{\mathbf{k}}(\mathbf{r},t) \equiv \phi_{\mathbf{p}}(\mathbf{r},t) = \frac{e^{i(\mathbf{p}+\mathbf{A}(t))\cdot\mathbf{r}}}{\sqrt{(2\pi)^3}} - c_H(\mathbf{p},t)\phi_H(\mathbf{r}) - c_L(\mathbf{p},t)\phi_L(\mathbf{r}). \tag{72}$$

Equation(72) is very similar to the Volkov states⁴ used to represent a free particle state in the presence of a vector potential. The terms c_H and c_L represent the effect of molecular potential on the ionized states and vanish for large values of kinetic momentum, and the scattering state becomes truly free. This is because c_H and c_L are decaying functions of $\mathbf{p} + \mathbf{A}(t)$ (see (61) and Eq.(62)). Assuming that the molecular potential does not significantly affect the energy of the scattering orbital, the corresponding energy for $\phi_{\mathbf{p}}(r,t)$ then can be approximated as only due to the free part,

$$E_{\mathbf{p}}(t) = \frac{1}{2} |\mathbf{p} + \mathbf{A}(t)|^2. \tag{73}$$

 $E_{\mathbf{p}}(t)$ represents the kinetic energy of ionized electron at time t dressed with IR pulse. Here the effect of the XUV field on the scattering electron is ignored since intensity of the XUV field is significantly lesser compared to that of the IR field. Using Eq. (72) in Eq.(8), we generate scattering states modified by the IR vector potential.

REFERENCES

¹G. Seabra, I. Kaplan, V. Zakrzewski, and J. Ortiz, The Journal of chemical physics **121**, 4143 (2004).

²B. Mignolet, R. Levine, and F. Remacle, Physical Review A **86**, 053429 (2012).

³C. Melania Oana and A. I. Krylov, The Journal of chemical physics **127**, 234106 (2007).

⁴M. Y. Ivanov, M. Spanner, and O. Smirnova, Journal of Modern Optics **52**, 165 (2005).